

Modeling of interfacial momentum exchange for wall-bounded bubbly flows

Jungwoo Kim¹, Dongjoo Kim², Hyungmin Park³ and Jun Ho Lee³

¹ Department of Mechanical System Design Engineering, Seoul National University of Science and Technology, Seoul, Korea

² Department of Mechanical Engineering, Kumoh National Institute of Technology, Gumi, Korea

³ School of Mechanical and Aerospace Engineering, Seoul National University, Seoul, Korea

ABSTRACT

The two-fluid model based on Eulerian-Eulerian approach has been widely used for simulating two-phase flows in industrial applications due to much less CPU requirement as compared to interface tracking methods. However, the two-fluid approach needs accurate modeling for interfacial mass, momentum, and heat transfers between phases. The important interfacial momentum exchange terms include drag, shear-induced lift, and wall-induced lift forces. In particular, it is important to accurately model the wall effect in order to predict ‘wall peaking’ or ‘core peaking’ phenomena observed in bubbly pipe flow. However, the wall effect is not fully understood yet and wall force coefficient in previous studies has a wide range of values, probably tuned to the experimental results. Therefore, to improve the performance of the two-fluid model for the bubbly flows, we are to propose a new model considering the wall effect on drag and lift forces. To do so, we separately perform resolved simulations for the flow around a moving sphere located near the wall. To evaluate the accuracy of the present model, numerical simulations based on two-fluid models are conducted for laminar bubbly flows available in the literature. The radial distributions of void fraction, liquid velocity, and bubble velocity show a reasonably good agreement with those from available numerical and experimental results.

KEYWORDS: Two-fluid model, laminar bubbly flows, wall effects, relative velocity

1. INTRODUCTION

Wall-bounded bubbly flows are frequently observed in many natural phenomena and engineering problems. In order to estimate the two-phase flows, the two-fluid model based on Eulerian-Eulerian approach [1, 2] is commonly used in industrial applications due to much less CPU requirements as compared to interface tracking method. In this approach, the balance equations for mass, momentum and energy are defined for each phase (which can be either liquid or gas) separately while weighted by the corresponding volume fraction. The exchange of mass, momentum and energy between the phases is described by several closure models such as drag, shear-induced lift, wall-induced force and so on. So, the development of the accurate closure models is crucial in numerical simulations of two-phase flow problems [3]. Especially, the shear-induced lift and wall-induced force play an important role of determining the distribution of void fraction in wall-bounded bubbly flows. The shear-induced lift is generated due to the interaction of the bubble with the shear field of the liquid. In the presence of the shear-induced lift, the bubble

could move perpendicular to the liquid phase. Generally, the small bubble tends to move towards the wall, whereas the large bubble is pushed away from the wall. On the other hand, the wall-induced force pushes the bubbles away from the channel to prevent them touching the wall. As a result, the local positions of the bubbles in the wall-bounded flows are determined by the balance between the shear-induced lift and wall-induced force. In that respect, many studies have been conducted to develop more reliable models for the shear-induced lift and wall-induced force [4, 5]. Recently, Tomiyama et al. [6] proposed a closure model of the shear-induced lift, which has been confirmed by the recent experiments [3, 6]. On the other hand, only a few studies have been done about the wall effect on the lift [7]. Hence, the accurate modeling of the wall-induced force has not been yet established. Therefore, the objective of this study is to develop more accurate and reliable modeling of the wall-induced force and to verify its accuracy as compared to experimental data available in the literature.

Although the flow is likely to be turbulent in many cases of practical interest, in turbulent bubbly flows it is not simple to accurately evaluate the performance of the wall-induced force itself due to the uncertainty coming from a turbulence model. In that respect, as previously done by Antal et al. [8], Azpitarte and Buscaglia [9] and Lu et al. [10], laminar bubbly flows would be considered as the first step of evaluating the performance of the proposed wall-induced forces.

2. TWO-FLUID MODELS

For the simulation of bubbly flows, the governing equations for two-fluid models based on Eulerian-Eulerian approach are considered.

$$\frac{\partial(\alpha_q \rho_q)}{\partial t} + \nabla \cdot (\alpha_q \rho_q \bar{u}_q) = 0, \quad (1)$$

$$\frac{\partial(\alpha_q \rho_q \bar{u}_q)}{\partial t} + \nabla \cdot (\alpha_q \rho_q \bar{u}_q \bar{u}_q) = -\alpha_q \nabla p + \alpha_q \rho_q \bar{g} + \nabla \cdot \bar{\tau}_q + \bar{M}_q. \quad (2)$$

Here, α_q is the volume fraction of q-th phase (liquid (L) or gas (G) phase). ρ_q and \bar{u}_q are the density and velocity component of each phase, respectively. Also, p and $\bar{\tau}_q$ are the pressure and viscous stresses, respectively. \bar{M}_q is the interfacial momentum exchange terms such as drag, shear-induced lift and wall-induced forces. Those are modeled considering that the gas phase has the form of dispersed bubbles, which will be later explained in detail. Because laminar bubbly flows are considered in this study, the turbulent dispersion force is neglected among the interfacial momentum exchange terms.

3. MODELING OF INTERFACIAL MOMENTUM EXCHANGE

3.1 Drag

The drag model proposed by Ishii and Zuber [11] is considered as

$$\bar{M}_G^{drag} = -\bar{M}_L^{drag} = -\frac{3}{4} \frac{\alpha_G}{d_b} C_D \rho_L (\bar{u}_G - \bar{u}_L) |\bar{u}_G - \bar{u}_L|, \quad (3)$$

where C_D is the drag coefficient. Ishii and Zuber [11] proposed $C_D = \frac{24}{\text{Re}_b}(1 + 0.1\text{Re}_b^{0.75})$

($\text{Re}_b = \frac{\rho_L |\bar{u}_G - \bar{u}_L| d_b}{\mu_m}$, $\mu_m = \frac{\mu_L}{1 - \alpha_G}$) for bubbly flows. Also, d_b is the diameter of the bubbles. Here, subscript b means bubble.

3.2 Shear-induced lift

When the local liquid velocities experienced by the bubble are asymmetrical, the local pressure distribution at the bubble surface also becomes asymmetrical. This results in a net force (called lift force) acting on the bubble in the direction perpendicular to the motion of the bubble relative to the liquid. Therefore, it requires the modeling of the shear-induced lift in order to estimate the lateral motion of the bubble. The lift force is correlated to the relative velocity and the local liquid vorticity as

$$\bar{M}_G^{lift} = -\bar{M}_L^{lift} = C_L \alpha_G \rho_L (\bar{u}_L - \bar{u}_G) \times (\nabla \times \bar{u}_L). \quad (4)$$

Here C_L is the lift factor and ranges from about 0.01 to 0.5 [12].

The recent numerical and experimental studies [6, 13] showed that the sign of the direction of the lift force is changed if a bubble experiences deformation. The lift factor with constant value which has been commonly used in two-fluid models cannot explain the change in the direction of the lift force. In that respect, in this study, the model proposed by Tomiyama et al. [6] showing the change in the direction of the lift force with respect to the bubble size is used to consider the shear-induced lift.

In the correlation of Tomiyama et al. [6], C_L is given as a function of Reynolds number and Eotvos number as below.

$$C_L = \begin{cases} \min[0.288 \tanh(0.121 \text{Re}_b), f(Eo)] & Eo < 4 \\ f(Eo) & 4 \leq Eo \leq 10 \\ -0.29 & Eo > 10 \end{cases} \quad (5)$$

$$f(Eo) = 0.00105 Eo^3 - 0.159 Eo^2 - 0.0204 Eo + 0.474 \quad (6)$$

Here, the Eotvos number is defined as $Eo = \frac{g(\rho_L - \rho_G)d_H}{\sigma}$, $d_H = d_b(1 + 0.163 Eo^{0.757})^{1/3}$. σ is the surface tension.

3.3 Wall-induced force

When the bubbles are moving close to a wall, the drag and lift forces acting on the bubble become different from the drag and shear-induced forces explained in the above. Therefore, to account for the wall effect on the drag and lift, additional interfacial momentum exchange terms are required.

For the modification of the force in wall-normal direction (usually called wall-lubrication or wall-repulsion force), the model proposed by Antal et al. [8] is usually considered.

$$\bar{M}_G^{lift,wall} = -\bar{M}_L^{lift,wall} = \frac{2\alpha_G \rho_L U_R^2}{d_b} (C_{w1} + C_{w2} \frac{d_b}{y_w}), \quad (7)$$

with $C_{w1} = -0.104 - 0.06|U_R|$, $C_{w2} = 0.147$. Here, U_R is the relative velocity between the liquid and gas phases. y_w is the distance from the wall boundary.

However, Rzehak et al. [5] mentioned the correlation of Antal et al. [8] showed a little low value close to the wall. In bubbly flows, the peak position of the void fraction is determined by the balance between the shear-induced lift and wall-induced lift. So, if the wall-induced lift is underestimated, void fraction profiles are biased toward the wall. Therefore, in this study, following Antal et al. [8]'s study, separate numerical simulations for a sphere moving near the wall are performed in order to improve the accuracy of the wall-induced lift near the wall (for more details, see Appendix A).

Based on the simulation results, a modified wall-induced lift is proposed as below.

$$\overline{M}_G^{lift,wall} = -\overline{M}_L^{lift,wall} = \frac{2\alpha_G \rho_L U_R^2}{d_b} (C'_{w1} + C'_{w2} \frac{d_b}{y_w} + C'_{w3} (\frac{d_b}{y_w})^2 + C'_{w4} (\frac{d_b}{y_w})^3 + C'_{w5} (\frac{d_b}{y_w})^4), \quad (8)$$

with $C'_{w1} = 0.01$, $C'_{w2} = -0.125$, $C'_{w3} = 0.355$, $C'_{w4} = -0.335$, $C'_{w5} = 0.1358$. This correlation is only valid for $y_w/d \geq 0.5$ because for $y_w/d < 0.5$ bubbles could not be present. So, in this study for $y_w/d < 0.5$ $\overline{M}^{lift,wall}(y/d_w) = \overline{M}^{lift,wall}(y/d_w = 0.5)$.

Figure 1(a) shows the distribution of the present wall-induced lift along the radial direction. For comparison, those by Antal et al. [8] and Krepper et al. [14] are also included.

On the other hand, in order to also modify the drag on the bubbles near the wall, the wall-induced drag is also modeled as follows:

$$\overline{M}_G^{drag,wall} = -\overline{M}_L^{drag,wall} = \frac{2\alpha_G \rho_L U_R^2}{d_b} (C'_{w1} + C'_{w2} \frac{d_b}{y_w} + C'_{w3} (\frac{d_b}{y_w})^2 + C'_{w4} (\frac{d_b}{y_w})^3 + C'_{w5} (\frac{d_b}{y_w})^4), \quad (9)$$

with $C'_{w1} = 0$, $C'_{w2} = 0.0074$, $C'_{w3} = -0.0832$, $C'_{w4} = 0.1386$, $C'_{w5} = -0.0283$. Similar to the lift force, for $y_w/d < 0.5$ $\overline{M}^{drag,wall}(y/d_w) = \overline{M}^{drag,wall}(y/d_w = 0.5)$.

Although some researches such as Moraga et al. [15] mentioned the inclusion of the wall-induced drag, so far it is ignored in most of the studies based on two-phase models. However, as shown in Fig. 1(b), the inclusion of the wall-induced drag increases the total drag by 30% as compared to the drag ($C'_D \approx 1$ at $Re_b=100$) explained in Sec. 3.1, which could affect the bubble motion close to the wall. In that respect, in this study, to account for the wall effect on the bubble motion, the wall-induced drag is considered together with the wall-induced lift.

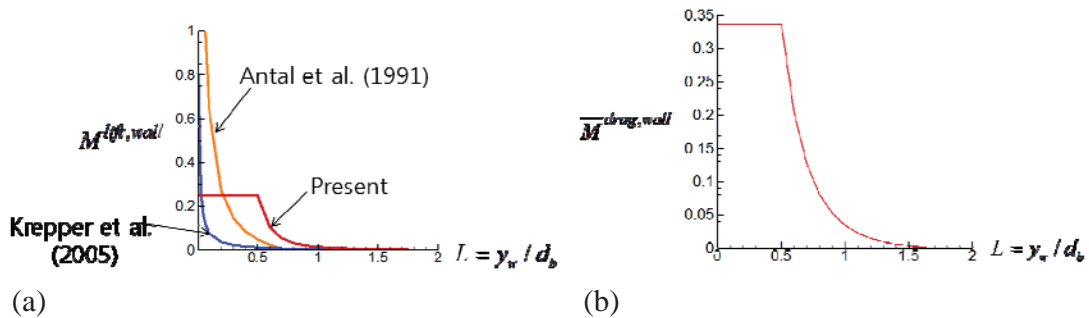


Figure 1. (a) $\overline{M}^{lift,wall}$ and (b) $\overline{M}^{drag,wall}$.

4. NUMERICAL RESULTS

In this study, the laminar bubbly flow studied by Nakoryakov et al. [16, 17] is considered in order to verify the accuracy of present modeling of interfacial momentum exchange, as previously done by Antal et al. [8]. The schematic diagram of the computational domain considered in this study is presented in Fig. 2(a). Also, table 1 shows the flow parameters in Nakoryakov et al. [16, 17]'s experiment. As shown in Fig. 2(b), the condition considered by Nakoryakov et al. [16, 17] belongs to bubbly flow regime [18]. The size of the computational domain is 75mm (r) \times 1200mm (y). The number of grid points used is 60 (r) \times 1200 (y). As the boundary conditions, in the inlet, parabolic velocity is used for water and the uniform velocity does for air. Also, the void fraction in the inlet is assumed to be uniform. On the other hand, at the exit, pressure boundary condition is given.

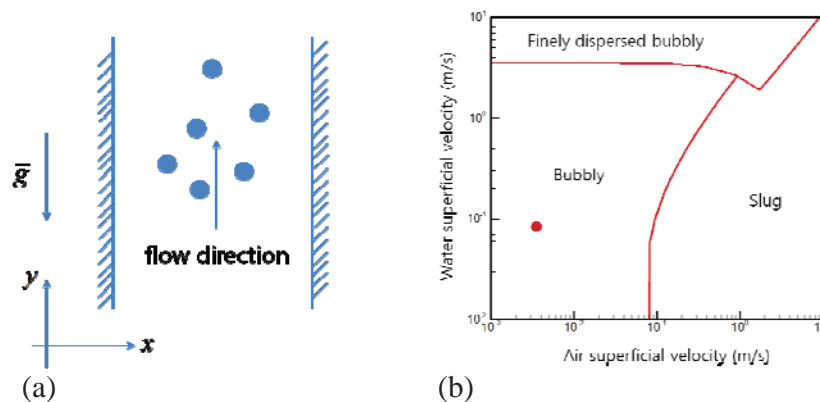


Figure 2. (a) Schematic diagram; (b) flow map.

Table 1. Experimental conditions performed by Nakoryakov et al. [16, 17]

| Liquid phase Reynolds number | Liquid velocity (m/s) | Pipe diameter (mm) | Bubble diameter (mm) | Average void fraction |
|------------------------------|-----------------------|--------------------|----------------------|-----------------------|
| 1276 | 0.0855 | 15 | 0.87 | 1.9% |

Figures 3 and 4 show the radial distribution of the void fraction, and liquid and gas velocities under the fully developed situations, respectively. For comparison, Nakoryakov et al. [16, 17]'s experimental data and the numerical results of Antal et al. [8] are included. In Antal et al. [8], it is adopted the shear-induced lift with the constant C_L of 0.1 and the wall-induced lift proposed by Antal et al. [8].

As shown Fig. 3, void fraction is almost flat in the interior, but has a peak near a wall. It is called "wall peaking". As well known, wall-peak location is decided by the balance between the shear-induced and wall-induced lift forces. The radial distribution of the interfacial momentum exchange terms considered in this study is presented in Fig. 5. In the correlation of Tomiyama et al. [6], the sign of C_L changes in terms of the bubble diameter. In air-water system, the critical bubble diameter is 5.8mm. So, under the present conditions, the sign of C_L is positive. Hence, as shown in Fig. 5, the shear-induced lift pushes the bubbles toward the wall. On the other hand, the wall-induced lift does them into the middle of the pipe. As shown in Fig. 1(b), its effect is

limited in the region close to the wall ($y < 2d_b$). As a result, the wall-induced lift goes to zero far away from the wall. So, the shear-induced lift also should become zero to balance with the wall-induced lift in that region.

As shown in Fig. 4, although the present study is laminar condition, the radial distribution of the liquid velocity is quite different from the parabolic velocity profile due to the presence of the bubbles. Due to large buoyancy forces near the wall, the velocity of the liquid velocity is increased as compared to that without bubbles. As a result, due to the continuity, the velocity of the liquid velocity near the core should become smaller than that without bubbles. Eventually, the velocity of the liquid phase is almost constant in the interior, enabling the shear-induced force nearly zero as shown in Fig. 5.

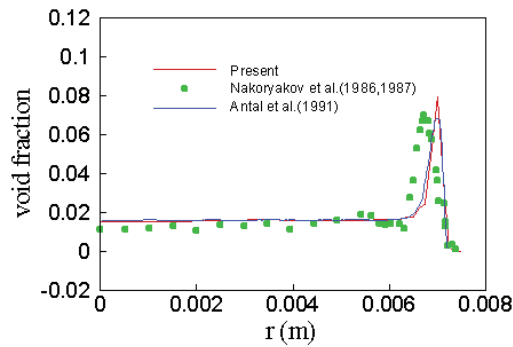


Figure 3. Void fraction in radial direction.

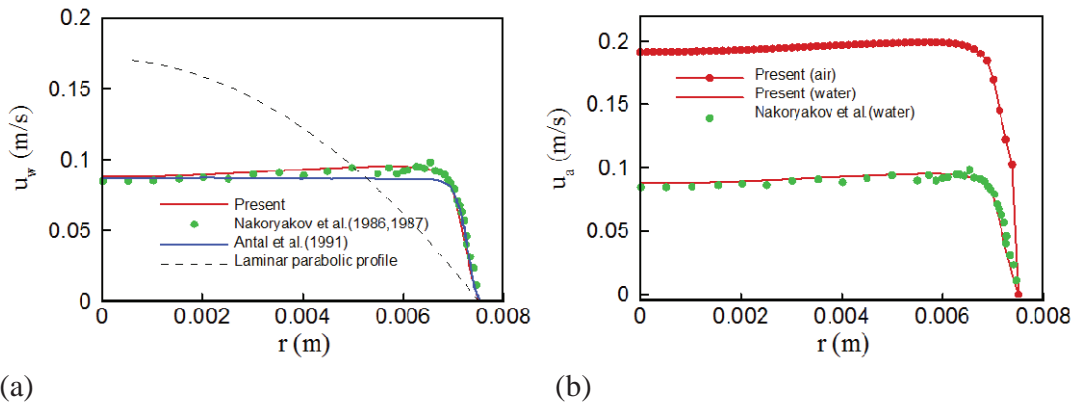


Figure 4. Distribution of (a) liquid (water) and (b) gas (air) velocities in radial direction.

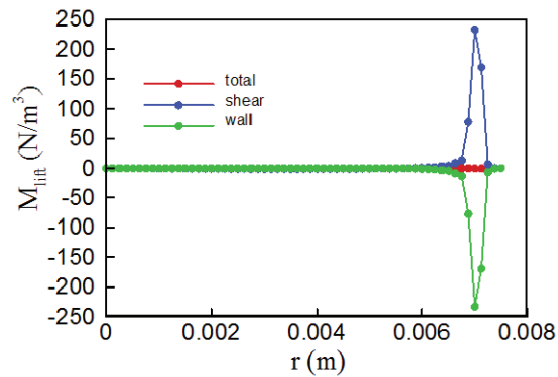


Figure 5. Radial distribution of the interfacial momentum exchange terms: $\overline{M}_{lift}^{lift}$ and $\overline{M}_{lift}^{wall}$.

Figure 6 shows the distribution of the relative velocities between liquid and gas phases in radial direction. Toward the wall, the relative velocity is decreased although it is almost constant except for the near-wall region, which is consistent to the fact observed by Lu et al. [10]'s direct numerical simulations. On the other hand, in the absence of the wall-induced drag, the relative velocity is constant very close to the wall.

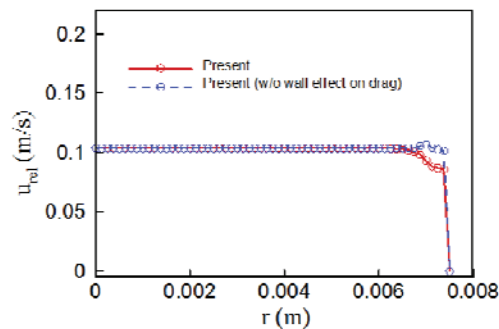


Figure 6. Distribution of the relative velocities between liquid (water) and gas (air) phases in radial direction.

5. CONCLUSIONS

The two-fluid model based on Eulerian-Eulerian approach is modified to improve its performance for the bubbly flows. To do so, we proposed a new model considering the wall effect on drag and lift forces while it is separately performed the resolved simulations for the flow around a moving sphere located near the wall as previously done by Antal et al. [8]. The simulation results provide us the change in the drag and lift forces acting on the sphere with respect to the distance between the sphere and the wall. To evaluate the accuracy of the present model, the numerical simulations based on the modified two-fluid models are conducted for laminar bubbly flows available in the literature [16, 17]. The radial distributions of void fraction, liquid velocity, and bubble velocity show a reasonably good agreement with those from available numerical and experimental results. Also, the relative velocity between continuous liquid and bubbles near the wall is better estimated as a result of considering the wall effect on drag. As a result, more accurate and reliable results for bubbly flows could be provided by the use of the

present proposed wall-induced drag and lift together with the shear-induced lift of Tomiyama et al. [6].

In the future work, the present results would be extended into pseudo-turbulence and fully turbulence cases.

ACKNOWLEDGMENTS

This study was supported by the National Research Foundation of Korea (NRF) grant funded by the Korea government (MSIP) (No. 2012M2A8A4055647).

REFERENCES

1. M. Ishii and K. Mishima, "Two-fluid model and hydrodynamic constitutive relations", *Nuclear Engineering and Design*, **82**, pp. 107-126 (1984).
2. B. J. Kim, J. Kim and K. D. Kim, "On the wall drag term in the averaged momentum equation for dispersed flows", *Nuclear Science and Engineering*, **178**, pp. 1-15 (2014).
3. D. Lucas, E. Krepper and H.-M. Prasser, "Use of models for lift, wall and turbulent dispersion forces acting on bubbles for poly-dispersed flows", *Chemical Engineering Science*, **62**, pp. 4146-4157 (2007).
4. T. Hibiki and M. Ishii, "Lift force in bubbly flow systems", *Chemical Engineering Science*, **62**, pp. 6457-6474 (2007).
5. R. Rzehak, E. Krepper and C. Lifante, "Comparative study of wall-force models for the simulation of bubbly flows", *Nuclear Engineering and Design*, **253**, pp. 41-49 (2012).
6. A. Tomiyama, H. Tami, I. Zun and S. Hosokawa, "Transverse migration of single bubbles in simple shear flows", *Chemical Engineering Science*, **57**, pp. 1849-1858 (2002).
7. A. M. Thomas, J. Fang, J. Feng and I. A. Bolotnov, "Estimation of shear-induced lift force in laminar and turbulent flows", *Nucl. Tech.*, **190**, pp. 274-291 (2015).
8. S. P. Antal, R. T. Lahey and J. E. Flaherty, "Analysis of phase distribution in fully developed laminar bubbly two-phase flow", *International Journal of Multiphase Flow*, **7**, pp. 635-652 (1991).
9. O. E. Azpitarte and G. C. Buscaglia, "Analytical and numerical evaluation of two-fluid model solutions for laminar fully developed bubbly two-phase flows", *Chemical Engineering Science*, **58**, pp. 3765-3776 (2003).
10. J. Lu, S. Biswas and G. Tryggvason, "A DNS study of laminar bubbly flows in a vertical channel", *International Journal of Multiphase Flow*, **32**, pp. 643-660 (2006).
11. M. Ishii and N. Zuber, "Drag coefficient and relative velocity in bubbly, droplet or particulate flows", *AIChE Journal*, **25** (5), pp. 843-855 (1979).
12. S. K. Wang, S. J. Lee, O. C. Jones, Jr and R. T. Lahey, Jr, "3-D turbulence structure and phase distribution measurements in bubbly two-phase flows", *International Journal of Multiphase Flow*, **13**, pp. 327-343 (1987).
13. R. Adoua, D. Legendre and J. Magnaudet, "Reversal of the lift force on an oblate bubble in a weakly viscous linear shear flow", *Journal of Fluid Mechanics*, **628**, pp.23-41 (2009).

14. E. Krepper, D. Lucas and H.-M. Prasser, "On the modelling of bubbly flows in vertical flows", *Nuclear Engineering and Design*, **235**, pp. 597-611 (2005).
15. F. J. Moraga, A. E. Larreteguy, D. A. Drew and R. T. Lahey, Jr., "A center-averaged two-fluid model for wall-bounded bubbly flows", *Computers and Fluids*, **35**, pp. 429-461 (2006).
16. V. E. Nakoryakov et al., "Study of upward bubbly flow at low liquid velocities", *Izv. Sib. Otdel. Akad. Nauk SSSR*, **16**, pp. 15-20 (1986).
17. V. E. Nakoryakov et al., "Study of downward bubbly flow in a vertical pipe", *Zh. Prikl. Mekh. Tekh. Phys.*, **1**, pp. 69-73 (1987).
18. T. Hibiki, M. Ishii and Z. Xiao, "Axial interfacial area transport of vertical bubbly flows", *International Journal of Heat and Mass Transfer*, **44**, pp. 1869-1888 (2001).
19. J. Kim, D. Kim and H. Choi, "An immersed-boundary finite-volume method for simulations of flow in complex geometries", *Journal of Computational Physics*, **171** (1), pp. 132-150 (2001).

APPENDIX A

In this appendix, the resolved simulations for the flow around a moving sphere located near the wall is presented to propose a new model considering the wall effect on drag and lift forces.

In this simulation, the immersed boundary method developed by Kim et al. [18] is used. Fig. A1 shows the computational domain and boundary conditions considered. Following Antal et al. (1991)'s approach, the bubble is assumed to be a sphere. The Reynolds number based on the speed and diameter of the sphere is 100, which is similar to that of bubbles (about 90) in Narkoyakov et al. (1986).

To propose a new model of wall-induced force, the formula derived by Antal et al. [7] is considered:

$$\overline{M}_G^{wall} = -\overline{M}_L^{wall} = \frac{2\alpha_G \rho_L U_R^2}{d_b} \left(C'_{w1} + C'_{w2} \frac{d_b}{y_w} + C'_{w3} \left(\frac{d_b}{y_w} \right)^2 + C'_{w4} \left(\frac{d_b}{y_w} \right)^3 + C'_{w5} \left(\frac{d_b}{y_w} \right)^4 + \dots \right).$$

In this study, to improve the accuracy of the wall-induced force, the terms up to fourth order are considered while Antal et al. [8] evaluated up to first order. The coefficients $C'_{w1} \sim C'_{w4}$ are determined by fitting the current numerical results.

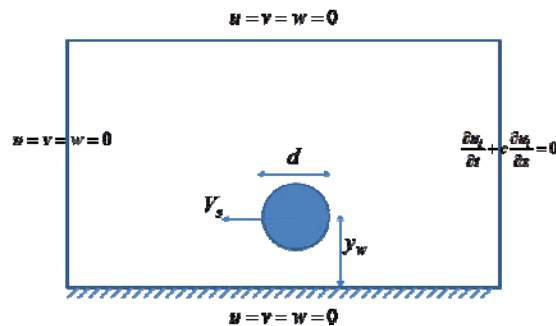


Figure A1. Computational domain and boundary conditions.